



OPEN

# A rapid approach for linear epitope vaccine profiling reveals unexpected epitope tag immunogenicity

Kirsten Browne-Cole<sup>1,5</sup>, Kyrin R. Hanning<sup>2,5</sup>, Kevin Beijerling<sup>2</sup>, Meghan Rousseau<sup>1</sup>, Jacelyn Loh<sup>3,4</sup> & William Kelton<sup>1,2</sup>✉

Antibody epitope profiling is essential for assessing the robustness of vaccine-induced immune responses, particularly while in development. Despite advancements in computational tools, high throughput experimental epitope validation remains an important step. Here, we describe a readily accessible method for rapid linear epitope profiling using phage-displayed oligo pools in combination with Nanopore deep sequencing. We applied this approach to TeeVax3, a Group A *Streptococcus* vaccine candidate, to investigate the antibody response generated in a pre-clinical rabbit model and assess antigen immunogenicity. Surprisingly, we found a strong bias in antibody binding response towards the N-terminal epitope tag used for purification. These tags are widely reported to have low immunogenicity and are frequently left uncleaved in pre-clinical studies. We further confirmed that the observed immune response against the epitope tag dominated even the conformational binding response and, using synthetic peptides, narrowed the epitope down to a set of 10 residues inclusive of the Histidine residues. Our findings highlight the importance of epitope-tag removal in pre-clinical studies and demonstrate the utility of rapid Nanopore sequencing for early-stage vaccine evaluation.

**Keywords** Vaccine profiling, Linear epitopes, Polyhistidine tag, TeeVax

Vaccine protection is strongly correlated with the quality and longevity of B and T cell responses induced against a given pathogen<sup>1–3</sup>. While T cell responses are driven by MHC loading of linear peptide epitopes present in vaccine antigens, antibodies can engage targets directly by binding to either linear epitopes or conformational epitopes formed when antigenic moieties are brought into close proximity by three-dimensional folding. Understanding the epitope distribution and binding affinity of the antibody response provides invaluable information for vaccine development efforts, especially where responses towards specific neutralizing epitopes are desired<sup>4,5</sup>. Alongside predictive computational tools<sup>6</sup>, several high-throughput wet lab approaches are widely used to profile the antigenic epitopes driving antibody responses<sup>7,8</sup>, particularly for applications in virology. These approaches can be adapted more widely to vaccine profiling<sup>9</sup>.

Crystallography remains the highest accuracy technique for antibody epitope mapping, followed by more recently developed Cryo-EM approaches<sup>10</sup>. Unfortunately, throughput is a challenge for these methods, and capturing a comprehensive snapshot of an antibody response against an antigen is very resource intensive. Instead, protein display systems have gained popularity as millions of individual epitope sequences can be physically linked to an underlying genotype that can be recovered by next-generation sequencing. Antigens can be expressed as full-length proteins or tiled as short peptides. The VirScan approach used phage display to present more than  $1 \times 10^8$  unique linear peptides from human viruses for capture by sera-derived antibodies from a global cohort of individuals<sup>11,12</sup>. In addition to antigen tiling, peptide sequences can also be systematically mutated using techniques like deep mutational scanning to provide greater precision when defining antibody epitopes<sup>13,14</sup>. The use of next-generation sequencing is particularly advantageous as it allows the detection of rare binding events at low frequencies, important when defining the binding ranges of polyclonal antibodies.

Here, we used a peptide phage display approach to investigate antibody responses elicited by TeeVax3<sup>15</sup>, a component of the multivalent vaccine candidate under development for Group A *Streptococcus* (Strep A)

<sup>1</sup>Te Aka Mātuatua School of Science, University of Waikato, Hamilton 3240, New Zealand. <sup>2</sup>School of Pharmacy and Biomedical Science, University of Waikato, Hamilton 3240, New Zealand. <sup>3</sup>Faculty of Medical and Health Sciences, University of Auckland, Auckland 1023, New Zealand. <sup>4</sup>Maurice Wilkins Centre for Molecular Biodiscovery, Auckland, New Zealand. <sup>5</sup>Kirsten Browne-Cole and Kyrin R. Hanning: co-authorship. ✉email: wkelton@waikato.ac.nz

infection. Despite longstanding development campaigns by academic and industry groups<sup>16</sup>, no vaccines have yet been approved for this pathogen, in part because of large strain diversity and the risk of autoimmune induction by surface antigens (e.g. M protein). By instead concatenating sets of five to seven T antigens from diverse strains into three recombinant proteins (e.g. TeeVax3: T6M-T2M-T25M-T23M-T4N), protective immunity was induced in small animal models of Strep A infection<sup>15</sup>. Further work characterizing the antibody response in mice and rabbits used phage-displayed Fab immune libraries to isolate and crystallize high-affinity Fab domains against the T antigen<sup>17</sup>. High-resolution epitope mapping of antibody repertoires is key to understanding the drivers of vaccine efficacy. Surprisingly, there appeared to be immunodominant conformational epitopes towards the N-terminus of some T antigens with unusual temperature-dependent accessibility at 37 °C.

To better understand antibody biases and binding distribution on the TeeVax3 antigen in high throughput, we created a bacteriophage-based method for the rapid profiling of linear epitopes using Nanopore sequencing. Applying our method to sera from TeeVax3 immunized rabbits revealed a strong bias towards the N-terminal TEV/6-His tag sequence that dominated even the conformational antibody binding response. While epitope tags are routinely removed from vaccines, including most but not all TeeVax3 animal experiments<sup>15,17</sup>, conventional wisdom suggests these peptides should possess low immunogenicity<sup>18,19</sup>. In many cases, these tags are left on vaccine antigens, especially through the early stages of in vivo profiling in animal models<sup>20–22</sup>. As well as providing an updated set of tools for linear epitope profiling, our finding provides a cautionary tale for those developing antigen-based vaccines requiring exogenous peptide tags for purification or antigen tracking.

## Results

### Construction of tiled TeeVax peptide libraries for phage display

To profile TeeVax3 linear epitopes in high throughput, we developed a phage-based peptide display approach to make use of rapid Nanopore sequencing (Fig. 1a). We first cloned short control peptides encoding the 6-His tag and a cyclic peptide mimetic of lipooligosaccharide derived from the pathogen *N. gonorrhea* (PEP-1)<sup>23</sup> into pAK200 phage display vectors<sup>24</sup>. These peptides were selected as high-affinity antibodies targeting them are readily available. ELISA analysis confirmed control phage binding to both PEP-1 (mAb 2C7<sup>25</sup>) and anti-His (HIS.H8) monoclonal antibodies above background helper phage binding (Fig. 1b, c). Having demonstrated the suitability of this system for the accessible display of short peptides, we next created a library of peptides from the 940 amino acid TeeVax3 antigen. Bioinformatic tiling was used to generate 308 sequences, each 20 amino acids in length and offset by three amino acids, except for a final tile with a two amino acid offset. To confirm the suitability of nanopore sequencing for tile identification, we further calculated the Levenshtein distances between all tiles in the library (Supplementary Fig. S1). We found a minimum edit distance of 16 within the library, corresponding to a required sequencing error rate of 26.3% for misidentification during binning. All tile sequences were back translated, adapter sequences added to the 5' and 3' ends, and the resulting library ordered as an oligo pool (Twist Biosciences). A single cycle of PCR was used to create the second strand of DNA for restriction enzyme cloning into pAK200 and phage production.

### Characterization of TeeVax3 peptide libraries by Nanopore sequencing

Prior to phage epitope profiling, we first confirmed the cloned library coverage using Nanopore sequencing. Plasmid DNA was isolated and cloned amplicons were removed by restriction enzyme digest to eliminate PCR amplification bias. We obtained  $\geq 1.4$  million reads from the library using a Q score cutoff of 15 (Supplementary Fig. S2a) with a median fragment length of 720 bp corresponding to the expected size for the digested fragment (Supplementary Fig. S2b). Reads were then binned into tiles via Minimap2. We again observed that 100% of the expected tiles were present, although individual tile frequencies within this pool ranged from 0.07 to 0.57% (Fig. 2a). Bacteriophage were then produced and immediately used to reinfect cells to gather the fraction of the library amenable to expression by phage. Clonal dropout at this step would lead to gaps in epitope coverage; therefore, nanopore sequencing was again used to re-evaluate tile frequencies. We again sequenced to a depth of  $\geq 1.4$  million reads and saw 100% retention of tile coverage in the phage library. Here, we observed minor differences in tile frequency and a general broadening of the tile abundance distribution when compared to Round 0 (Pre-expression plasmid sequence pool) (Fig. 2b, c). Individual tile frequencies ranged from 0.036% to 1.82% indicating some expression biases but this was not concentrated to any one region of the antigen.

### Linear epitope profiling by multi-round phage display reveals significant binding to the N-terminal epitope tag

To enrich antigen-specific clones from the antibody repertoire of rabbits immunized with TeeVax3, we first purified a TeeVax3-specific pool of antibodies by immunoprecipitation. High-purity TeeVax3 antigen (Fig. 3a, Supplementary Figure S3a) was conjugated to agarose beads to enable the isolation of both linear and conformational TeeVax3 epitope-binding clones. This process yielded approximately 1.3 mg of TeeVax3-specific antibodies per mL of immunized rabbit sera. SDS PAGE confirmed a high purity of the resulting antibody fraction with multiple bands representing heavy and light chains from multiple antibody subclasses (Fig. 3b, Supplementary Figure S3b). Antibodies were also isolated from unimmunized sera by Protein G chromatography. Together, we used these polyclonal antibody pools to evaluate background binding to the TeeVax3 library phage (Fig. 3c). Polyclonal antibodies enriched for binding to TeeVax3 had 4.7-fold higher signal than the polyclonal pool from unimmunized individuals. However, the unimmunized pool did show low but consistent binding above background (uncoated control) of 1.3-fold. We then used the TeeVax3-specific antibodies directly for phage panning of the TeeVax3 linear epitope library. We performed three rounds of panning and used Nanopore sequencing to track the clonal enrichment of each tile. Enrichment scores were determined by calculating the ratio of observed tile frequencies from the pre-panned phage library and post-panned libraries.

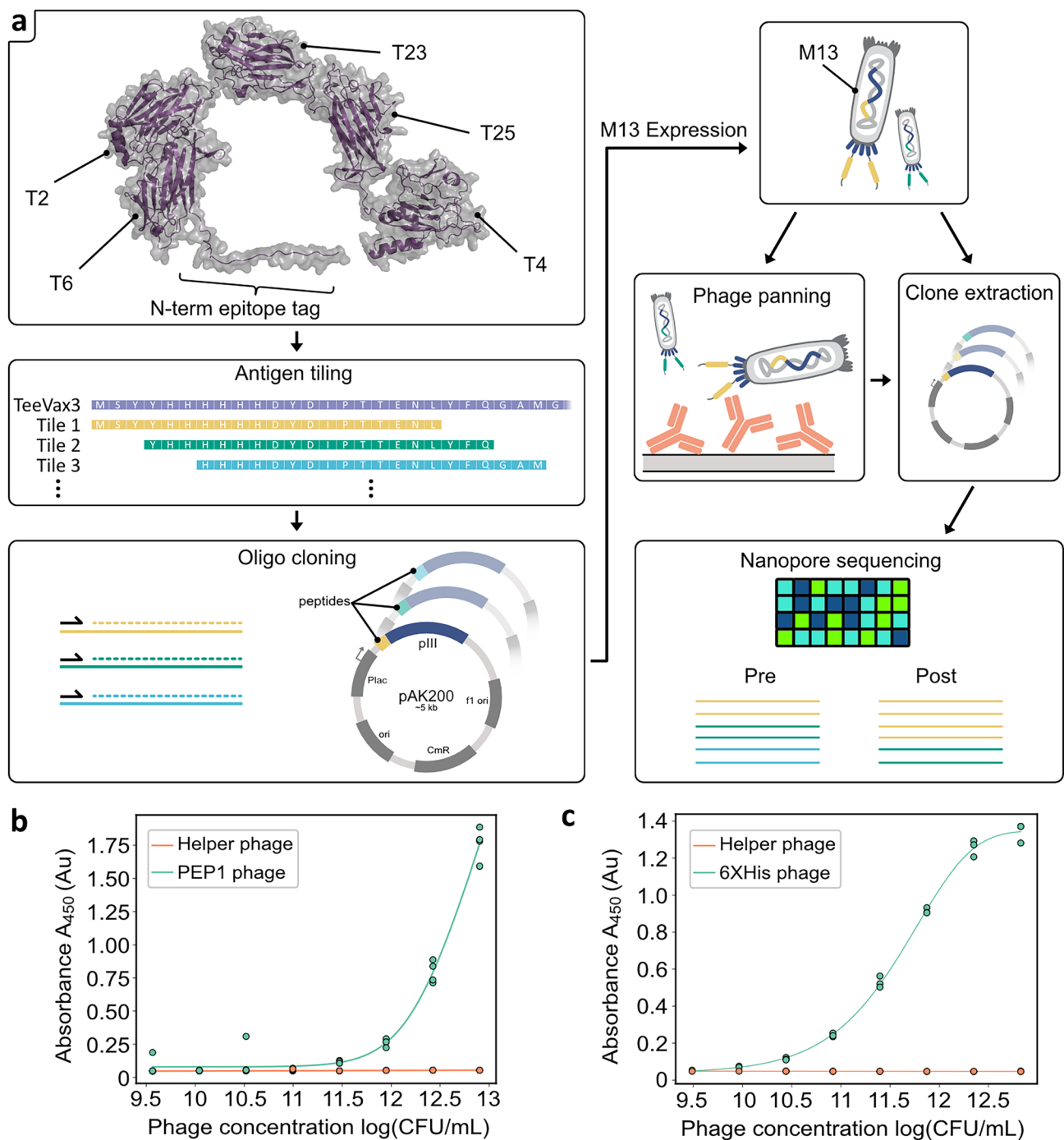


**Fig. 1.** Linear antibody epitope profiling using phage panning and Nanopore sequencing. **(a)** Overall experimental scheme. Target antigen sequences are tiled into discrete peptides and encoded as an oligonucleotide pool. After a single cycle of PCR to create the complementary strands, these sequences are cloned into pAK200 plasmids and expressed on the pIII domain of M13K07 bacteriophage. Peptide tile abundances before and after panning against the vaccine-specific antibody pool are determined by Nanopore sequencing and the ratio of these frequencies used to determine epitope enrichment. ELISA analysis demonstrated specific binding of control phage expressing model PEP1 cyclic peptides to the 2C7 monoclonal antibody ( $n = 4$ ) **(b)** and phage displaying a 6-His epitope tag peptide to the HIS.H8 monoclonal antibody ( $n = 3$ ) **(c)**. Helper phage with no peptide displayed were used as the negative control. Representative plots from independent replicates are shown with each point representing an individual datapoint.

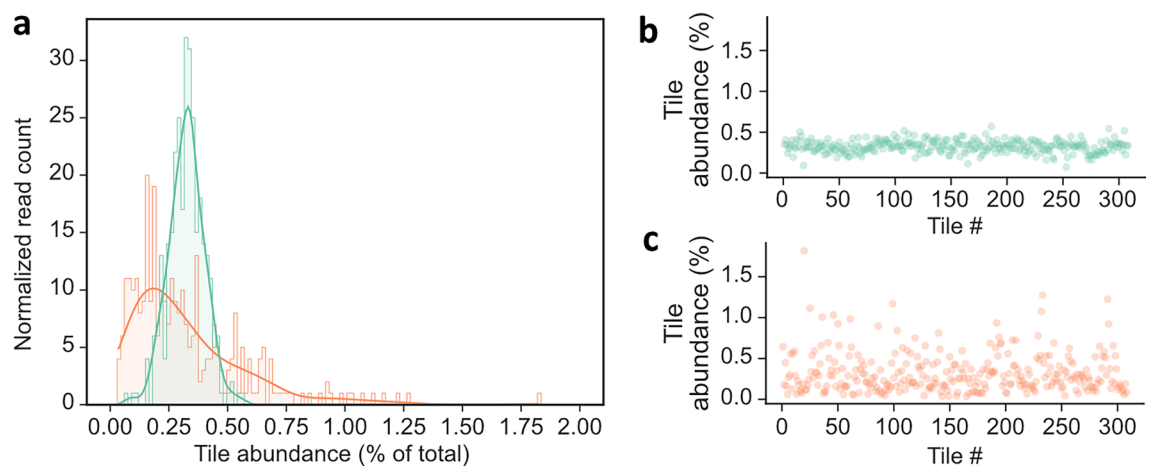


**Fig. 2.** Pre-panning peptide library evaluation by Nanopore Sequencing. **(a)** Distribution of individual tile abundances before (green) and after (orange) expression on phage, normalized to the total read count. Solid lines represent smoothed distributions generated by kernel density estimations of the underlying histogram plots. To determine whether expression bias is distributed evenly throughout the antigen, individual tile abundances were plotted against tile location within the antigen (Tile #) for **(b)** Round 0 pre-expression (green) and **(c)** Round 0 reinfected post-expression phage (orange).

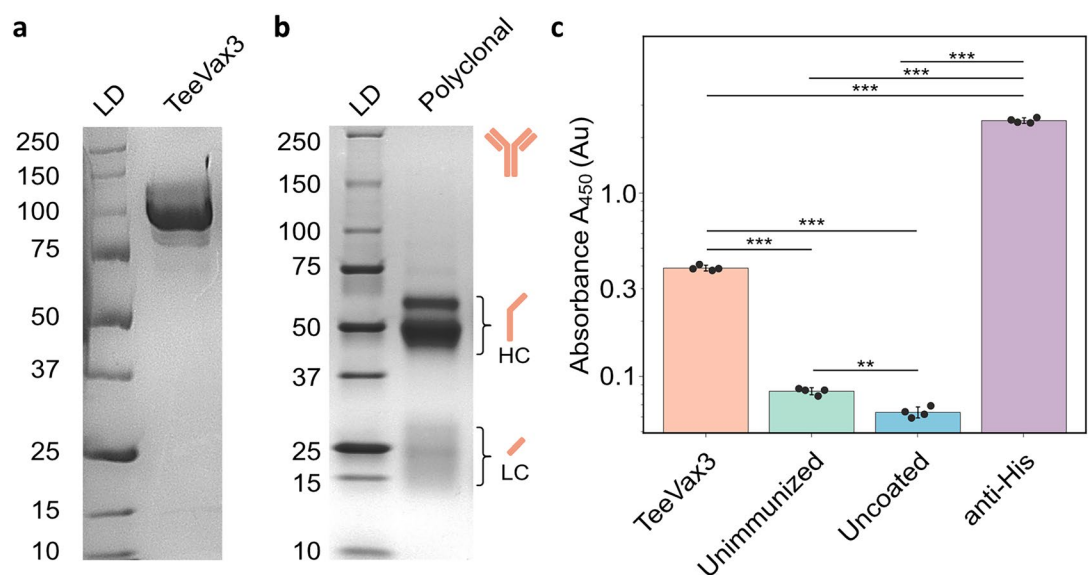


**Fig. 3.** Expression of TeeVax3 antigen and isolation of vaccine-specific antibodies. **(a)** TeeVax3 was expressed in *E. coli*, purified via Ni-NTA affinity chromatography and analyzed by reducing SDS-PAGE. **(b)** A custom chromatographic resin was created by conjugating TeeVax3 antigen to aldehyde-activated agarose beads and used to purify polyclonal antibodies from TeeVax3-immunized rabbits. Separation by reducing SDS-PAGE gel shows the various heavy chain and light chain sizes expected from a diversity of clonal sequences and antibody subclasses. **(c)** ELISA analysis of background binding of polyclonal antibodies to phage libraries. The plates were coated with polyclonal anti-TeeVax3, antibodies isolated from unimmunized serum by protein G chromatography, and anti-His (HIS.H8) as a positive control. Background signal was evaluated by measuring binding to plates blocked with PBS containing 2% w/v skim milk powder. Data shown is a representative plot with individual datapoints as each well in the plate ( $n = 4$ ). Pairwise t-tests with a Bonferroni correction applied for multiple comparisons were used to assess statistical significance (\*\* $p < 0.001$ , \*\* $p < 0.01$ , \* $p < 0.05$ ).

Over 64,000 high-quality sequences were obtained from phages after each round of panning, representing a greater than 200-fold coverage of the theoretical library diversity. We observed a rapid bias in representation towards tiles from the N-terminus of the TeeVax3 antigen corresponding to the 6-His epitope tag and TEV cleavage sequences (Fig. 4a). By round two of panning, the phage library sequence pool was dominated by 81.1%

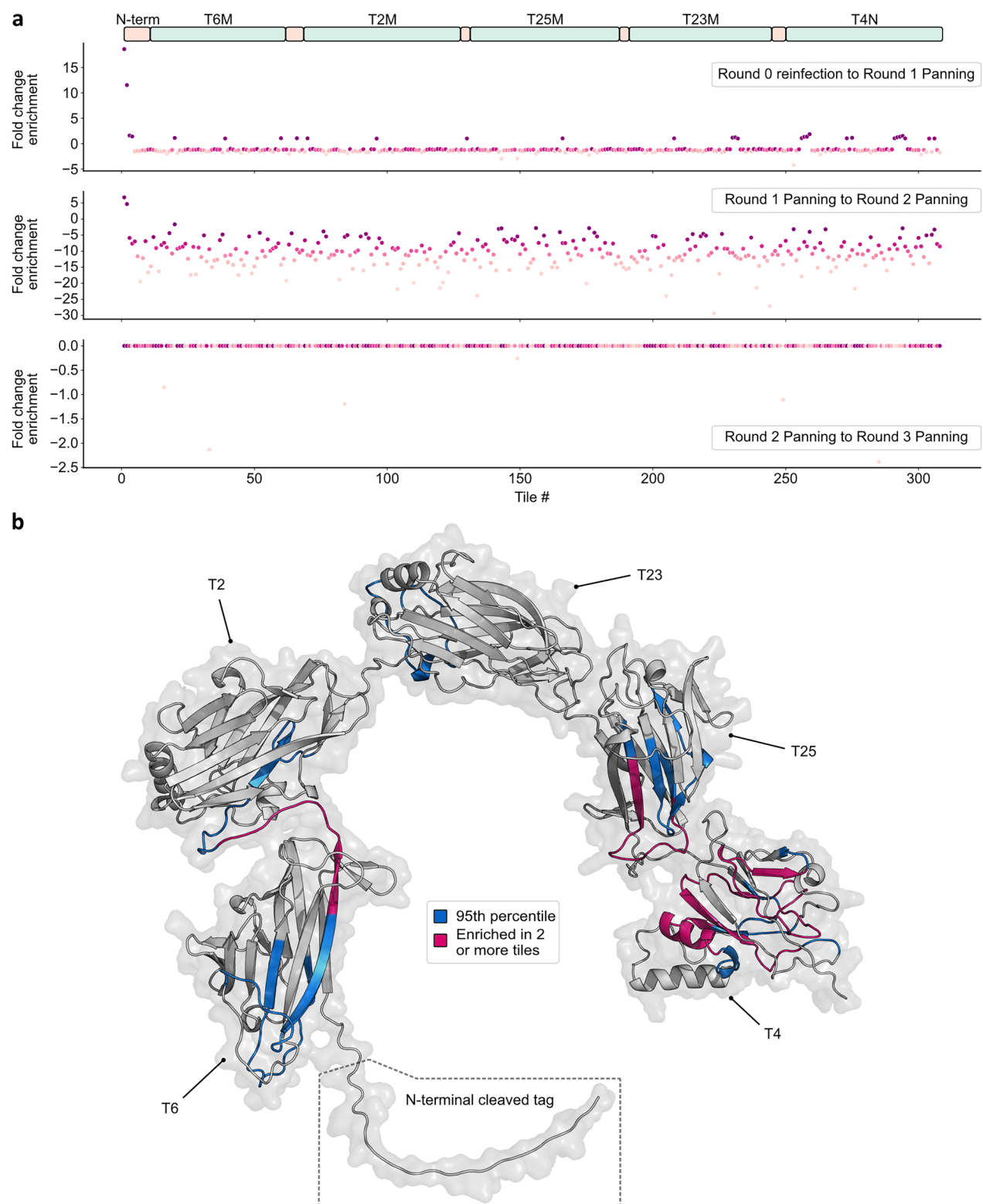


**Fig. 4.** Tile enrichment during panning against TeeVax3-specific antibody pool. **(a)** The TeeVax3 peptide pool was expressed on bacteriophage and panned against immobilized anti-TeeVax3 polyclonal antibodies. Fold enrichment values for each peptide tile were computed by dividing the post-panning frequency by the corresponding pre-panning frequency following Nanopore sequencing. Each data point represents an individual peptide tile sequence. **(b)** After excluding high abundance N-terminal tiles 1–3 as indicated in the dashed box, tiles above the 95th percentile were mapped to a model of TeeVax3. Blue indicates tiles above the 95th percentile and magenta shows sequences represented in two or more tiles.

of tile 1 (MSYYHHHHHHHDYDIPTTENTL) and 9.5% of tile 2 (YHHHHHHHDYDIPTTENLYFQ). Little further enrichment was observed in the third round of panning. We next explored the likelihood these sequences were the result of expression bias by comparing the enrichment of these tiles between the Round 0 pre-expression plasmid library and Round 0 reinfected post-expression frequencies. We found that while the proportion of tile 1 increased from 0.347 to 0.645% (1.9-fold), indicating a positive expression bias, tile 2 dropped in abundance from 0.404 to 0.176% (0.44-fold) indicating expression of this sequence was relatively disfavored. In each case, the > 10-fold enrichment of these sequences over the first round of panning far exceeds expression bias contributions. More broadly, we observed a decrease in the median tile frequency from 0.328% to 0.260% across all the tiles.

To further investigate clonal bias outside of the N-terminal sequences, we expanded the analysis between the Round 0 reinfected library and Round 1 of panning to include tiles with enrichment in the 95th percentile exclusive of tiles 1–3. These enriched peptides were mapped onto a three-dimensional representative model of the TeeVax3 antigen, generated using AlphaFold2<sup>26</sup> in the absence of crystal structure data (Supplementary Fig. S4). This process revealed a lack of antibody binding preference for the T2M domain, T25M domain, and the inter-domain spacer regions, except for the linker between the T6M and T2M domains. Instead, we observed some preference for T6M, T23M, and increasingly T4N binding where a high proportion of overlapping tiles were mapped (Fig. 4b).

### High-resolution epitope profiling defines a high-affinity peptide within the epitope tag

There remained the possibility that the unexpected binding we observed for the epitope tag could be a small fraction of the total antibody pool with most of the response being dominated by conformational epitope binders rather than linear epitope binders. To measure the relative abundance of linear epitope tag binders to all TeeVax3 antigen binders, against both conformational and linear epitopes, we cleaved the His tag from TeeVax3 using TEV protease and confirmed the absence of the His/TEV tag by ELISA using anti-His HRP for detection (Fig. 5a). ELISA analysis was then used to measure the relative anti-TeeVax3 antibody signal from purified sera samples with and without the His/TEV tag. We observed a decrease in antibody EC<sub>50</sub> (6.3-fold) upon removal of the epitope tag indicating the binders to Tiles 1 and 2 dominated the pool of antibodies against the antigen even with conformational binding clones present (Fig. 5b).

The unexpected immunogenicity of the epitope tag led us to profile the specific amino acids driving the antibody response with greater precision. We ordered a series of synthetic biotinylated peptides of decreasing size beginning with the 17 amino acids overlapping in Tiles 1 and 2 that provided the greatest enrichment by phage panning. Subsequent peptides reduced the size of this epitope with the smallest fragment tested consisting of a 7 amino acid sequence encompassing the 6-His tag (Fig. 6a). The peptides were captured with neutravidin and TeeVax3-specific antibodies were assayed for binding. We found the highest relative signal with the longest 17 amino acid epitope and a trend of similar binding for each of the 14-mer, 13-mer, and 10-mer tiles (Fig. 6b). A substantial drop in signal was observed for the shortest tile covering the 6-His tag with an additional Tyrosine motif. This dataset suggests the strongly immunogenic motif we observe encompasses both residues from the Histidine epitope tag and the TEV linker regions.

## Discussion

High-throughput epitope mapping tools provide a rapid snapshot of antibody binding bias against vaccine or pathogen antigens. In this study, we explored the use of Nanopore sequencing to rapidly profile linear epitope antibody binders derived from rabbit sera against the TeeVax3 candidate vaccine for Group A Streptococcus.

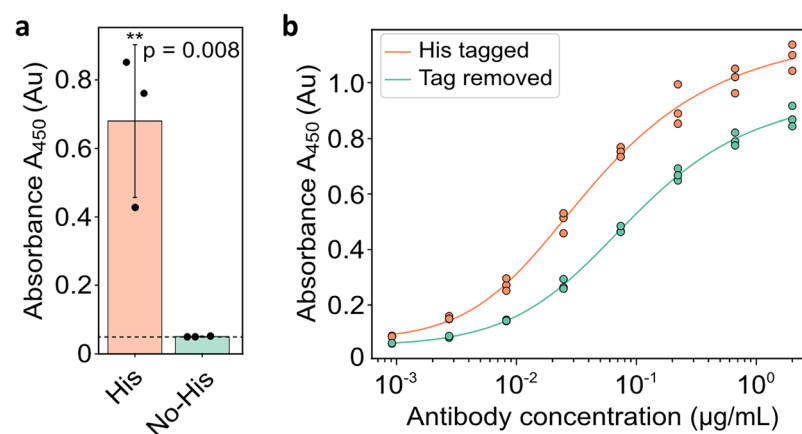


**Fig. 5.** Antibody response with and without the N-terminal epitope tag sequence. **(a)** TeeVax3 antigens were digested with TEV protease and the presence of residual Histidine epitope tag was assayed by single-well ELISA relative to the undigested antigen. The dashed line indicates background binding in the assay. Data are presented as the mean  $\pm$  SD ( $n=3$ ) and a pairwise t-test was performed to calculate the p-value ( $p=0.008$ ). **(b)** Representative ELISA plot showing polyclonal antibody responses towards TeeVax3 antigen with and without the epitope tag removed ( $n=3$ ). Each point represents an individual datapoint.

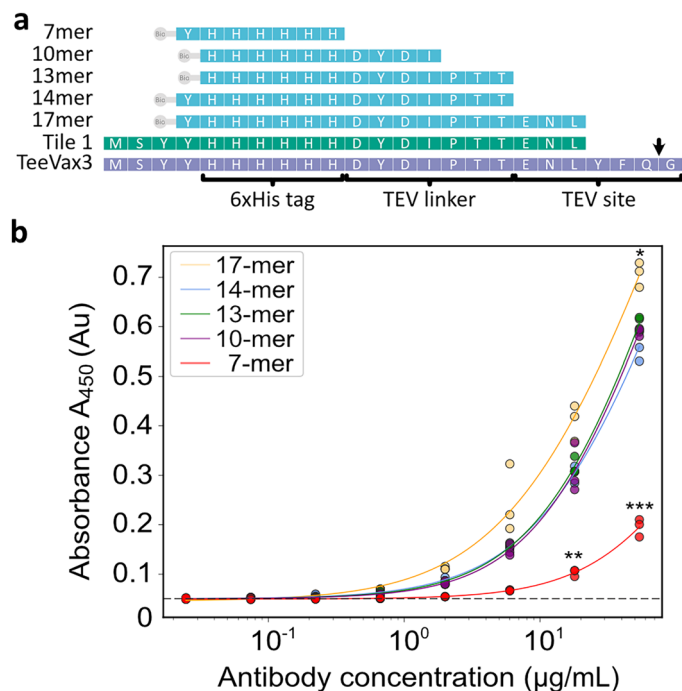


**Fig. 6.** Fine epitope profiling with synthetic peptides. **(a)** Peptide series with N-terminal biotin fusions generated from the Tile 1 TeeVax3 sequence. **(b)** ELISA analysis measuring the binding capacity of polyclonal TeeVax3-specific antibodies against biotinylated peptide series. The dashed line represents the average background signal obtained from negative wells ( $n=4$ ) where the polyclonal TeeVax3 antibodies were omitted. Pairwise t-tests were used for pairwise comparison at each concentration with Bonferroni correction for multiple comparisons (\*\* $p < 0.01$ , \*\*\* $p < 0.001$ , \* $p < 0.05$ ). A representative plot from independent replicates is shown with each point representing an individual datapoint.

This sequencing approach can have higher error rates than other next-generation sequencing approaches, such as Illumina, but we reasoned that the unique offset nature of the peptide tiles enables identification regardless of sequencing error. To develop the method, an oligo pool was ordered and used to create a library of 20-mer peptides derived from the TeeVax3 antigen. We then used a multi-round phage panning approach against enriched TeeVax3-specific polyclonal antibodies to monitor the enrichment of the expressed tiled peptides. After three rounds of panning, the resulting libraries were dominated by peptide tiles stemming from the N-terminus. We were surprised to find a strong enrichment of peptide sequences encoding the 6 His/TEV purification tag and therefore evaluated the relative binding signal of antibodies against the TeeVax3 antigen with and without epitope tag cleavage. This analysis confirmed the polyclonal pool was dominated by linear binders to sequences from the epitope tag and confirmed the unexpected immunogenicity observed by phage panning. To further understand the scope of the immunogenic epitope, we ordered a series of biotinylated peptides of decreasing size and observed binding even for the 6-His tag with one additional residue. Our findings indicate the residues displaying the strongest immunogenicity lie within a 10 amino acid sequence covering the 6-His epitope tag and the N-terminus of the TEV linker sequence.

Prior studies have used sequencing approaches with very low error rates, such as Illumina<sup>27,28</sup>, for linear epitope binding antibody mapping. The accessibility and speed of Nanopore allows for in-laboratory sequencing even if core facilities or next-generation sequencing providers are not readily available. Despite a high error rate, we found the sequence distance generated by offset peptide tiles was sufficient for accurate binning and determination of Nanopore read counts required to calculate enrichment factors. While we have used only a limited set of peptide tiles here (308) relative to other examples in literature<sup>29,30</sup>, the length of 20 amino acids means it is very unlikely sequencing errors could cause binning errors in larger libraries, with the exception of antigens with repeats or regions of high sequence homology. The finding that most antibody binders were directed to the epitope tag was unexpected, especially considering that His tags are typically considered to have low immunogenicity. While there are reports of His tags influencing antigen immunogenicity<sup>31,32</sup>, raising antibodies against His tags frequently requires conjugation to carrier proteins to elicit sufficient antibody titers<sup>33</sup>. It should be noted the strongest antibody binding signal we observed did require residues from the TEV cleavage site in addition to those from the 6-His tag. An obvious mitigation strategy is to remove the His tag via TEV cleavage, but this step is inconsistently performed in preclinical vaccine studies. The generation of non-productive antibodies against epitope tags could impact observed vaccine efficacy in early phases. It is also worth mentioning that TEV cleavage leaves a residual serine residue (ENLYFQ(S)) that is not likely to be immunogenic by itself but could contribute to the development of a neoepitope.

The background binding of polyclonal antibodies to the library phage presents one potential source of error in the method presented here. While we sought to minimize this influence through pre-enrichment of the antibody pool by immunoprecipitation against TeeVax3 antigen, we recommend the inclusion of an experimental arm panned against unimmunized sera or an antibody isotype control to enable identification of these tile sequences. A further challenge with using multiple rounds of phage panning is the resulting enrichment of high expressing rather than high-affinity peptide clones. Sequences with a growth advantage can bias tile frequency and lead to the false positive identification of linear epitopes. Here, we took steps to mitigate this issue by monitoring tile abundance before and after phage expression as well as using synthetic peptides to validate our top N-terminal hits. We suggest a maximum of two rounds of panning are required to detect tile enrichment when using next-generation sequencing approaches, as strong binders rapidly dominate the library. Further, employing two rounds of panning could provide additional information on the relative affinity of interactions assuming a limited influence from expression bias. When we removed the high abundance epitope tag peptides from the analysis and mapped the remaining tiles above the 95th percentile, we found a small number of linear epitopes unevenly distributed across the TeeVax3 antigen. Previous work has also found biases in antibody binding to T-antigens upon immunization. Raynes et al., report conformational binders with a bias towards the N-terminal ends of T18.1 N-domains exposed in a temperature-dependent manner<sup>17</sup>. While these data are from a limited subset of T-antigens, it is clear further exploration of immunodominant motifs would be valuable for developing these proteins as vaccines.

Epitope mapping studies provide insights into immune response bias that inform antigen design in vaccines. Here, we identify the epitope tag on TeeVax3 as having unanticipated immunogenicity. Beyond the scope of the findings presented here, our method could be used to further profile larger peptide libraries or be generalized for the analysis of other bacterial or viral pathogens. For example, to establish TeeVax3 correlates of protection across all 21 known T antigen groups encoded by the *tee* gene from Group A Strep pathogens<sup>34,35</sup>. This data would best be paired with experimentally generated information on conformational epitope binding. Nonetheless, the method presented here provides an accessible and low-cost approach to linear epitope panning using tools available to most molecular biology laboratories.

## Methods

### Antigen purification

The TeeVax3 antigen was expressed in *E. coli* by adapting previously described methods<sup>15</sup>. Briefly, pROEXhtb vectors encoding TeeVax3 were transformed into BL21 (DE3) cells and cultures in exponential growth phase induced with 0.1 mM Isopropyl  $\beta$ -D-1-thiogalactopyranoside (IPTG). After overnight growth at 18 °C for 18 h, cell pellets were resuspended in Lysis buffer (50 mM Tris-HCl pH 8, 150 mM NaCl, 20 mM imidazole), sonicated using a Qsonica Q700 with a 417-A microtip (Total time: 3 min, pulse-on time: 1 s, pulse-off time: 1 s), and centrifuged at 14,000 g for 30 min at 4 °C to recover the supernatant. His tagged antigens were purified by Ni-NTA chromatography using 5 mL HisTrap HP columns (Cytiva) on a BioRad NGC FPLC. Non-specifically bound proteins were removed with 50 mM Tris-Cl pH 8, 150 mM NaCl, 20 mM imidazole and the antigen eluted with 50 mM Tris-Cl pH 8, 150 mM NaCl, 1 M imidazole. Amicon Ultra-15 10 kDa centrifugal filters (Merck Millipore) were used to concentrate the protein before size exclusion polishing with a S75 16/60 column (GE Healthcare) using 50 mM Tris pH 8, 150 mM NaCl. Samples were buffer exchanged into 1× Phosphate Buffered Saline (PBS) for storage and analysed by 12% SDS-PAGE gel electrophoresis. For His tag removal, TeeVax3 antigen was buffer exchanged into 20 mM Tris pH 7.5 and digested overnight at 4 °C with TEV Protease (NEB). Undigested antigen and digested His tags were captured by Ni-NTA chromatography as described above, taking the flowthrough fraction as the untagged antigen.

### Animal experiments

All animal experiments were approved by The University of Auckland Animal Ethics Committee (Approval #R1663) and were performed in the Vernon Jansen Unit at The University of Auckland. All methods and procedures were performed according to the regulations and standards of the University of Auckland. Experimental methods are reported in accordance with the ARRIVE guidelines. TeeVax3 immunized rabbit serum was obtained from a New Zealand white rabbit immunized subcutaneously with 100  $\mu$ g of recombinant protein emulsified 1:1 with incomplete Freund's adjuvant and boosted at 2 and 4 weeks. Control serum was obtained in parallel from an unimmunized individual. All animals were deeply anaesthetized at day 42 with 90 mg/kg of intravenous sodium pentobarbitone, and antiserum was collected by terminal blood draw.

### Antibody purification

Immunoprecipitation of TeeVax3-specific antibodies was performed by coupling TeeVax3 antigen to AminoLink Plus Coupling Resin (ThermoFisher). Eight mg of TeeVax3 antigen in 0.1 M sodium phosphate, 0.15 M NaCl, pH 7.2 coupling buffer were incubated with 2 mL of resin at 4°C overnight with gentle rotation. The following day, 5 mL of pH 7.2 PBS and 100  $\mu$ L of Cyanoborohydride Solution were added and the mixture rotated for 4 h at room temperature. Two mL of conjugated resin was added to a gravity flow column and sera diluted five-fold in PBS was passed through the column. The bound fraction was washed with PBS, eluted with 0.1 M glycine pH 3, and neutralized with 10% the solution volume of 1M Tris pH 9.0. Amicon Ultra-15 10 kDa centrifugal filters (Merck Millipore) were used for buffer exchange into PBS prior to purity analysis by SDS PAGE. Negative control antibodies from unimmunized rabbits were purified by Protein G chromatography. Sera from these animals was again diluted more than five-fold in PBS and passed through a 1 mL Protein G column (Cytiva). After washing with > 10 column volumes of PBS, the bound antibody pool was eluted with Glycine HCl pH 3.0, neutralized with 1 M Tris pH 9.0 and buffer exchanged into PBS following the method used for anti-TeeVax3 antibodies.

### Antigen tiling

The tile library was created computationally by splitting the 941 amino acid sequence of the Teevax3 antigen (Supplementary Table S1) into 308 segments each 20 amino acids long. These peptides were offset by three amino acids to ensure complete coverage of potential binding sites. Bioinformatics software (Geneious Prime) was then used to back translate the tiles into nucleotide sequences, followed by the addition of adaptors containing a coding sequence, peptide transport signal and restriction sites to both 5' and 3' ends (5' adaptor CGAGGG CCCAGCCGGCCATGGCCGAGGGT, 3' adaptor TCGGCCTCGGGGGCCA). The resulting 308 tiles of 105 nucleotides each were then ordered as a single oligo pool (Twist Bioscience). In parallel, we designed control oligo nucleotides flanked by the 5' and 3' adapters encoding the PEP1 cyclic peptide (TGCGGTCCGATCCCA GTGCTGGATGAAAACGGCCTGTTGCTCCGGGTCCGTGC) and 6-His epitopes (CATCACCATCACCA TCACGACTACAAAGACGATGACGACAAG).

### Phage construction and peptide expression

Oligos were duplexed by a single cycle of PCR using OneTaq® Quick-Load® 2X Master Mix with Standard Buffer (NEB). A reverse primer (5'-TGGCCCCCGAGGCC-3') was included at 0.2 µM in the reaction alongside 12 ng of oligo template and the following conditions were used: denaturation at 94 °C for 1 min, 1 cycle of elongation at 60 °C for 1 min, followed by final extension for 5 min at 68 °C. The double-stranded oligo pool was digested with SfiI restriction enzyme for 2 h at 50 °C. Digested fragments were cleaned using a QIAquick nucleotide removal kit (Qiagen) and DNA concentration was quantified using a DeNovix double-stranded Ultra sensitivity assay. The library was then ligated into SfiI digested pAK200 vector and bound to Monarch columns (NEB) after the addition of five volumes of 5 M Guanidine Hydrochloride containing 30% isopropanol. The sample was then washed with 10 mM Tris-HCl pH 7.5, 80% ethanol and eluted with ultra-pure water. Ligated plasmids were transformed into electrocompetent SS320 cells and plated to create the final library. Library glycerol stocks were grown at 37 °C from OD 0.1 to 0.4–0.6 in LB media supplemented with 20 µg/mL chloramphenicol. M13K07 helper phage were added at an MOI of 20× and the culture incubated without shaking for 1 h to allow infection. Kanamycin antibiotic was added (35 µg/mL) and peptide expression was induced with 1 mM IPTG before overnight growth to produce phage. Culture supernatants were filtered through 0.22 µm filters and phage were precipitated by adding 20% of the total volume of 20% PEG/2.5 M NaCl and incubating on ice for at least 30 min. Phage were centrifuged at 16,000 g, resuspended in 1× PBS and spun again twice more at 16,000 g changing the tube between spins. Titers were quantified by spectrophotometry (DeNovix DS11) using the formula  $\text{virions/mL} = (A_{269} - A_{320}) \times 6 \times 10^{16} / (\text{phage ssDNA bases})^{36}$ .

### Control peptide phage ELISA analyses

ELISA plates were coated with 50 µL volumes of Sodium Carbonate buffer pH 9.6 (34 mM NaHCO<sub>3</sub>, 16 mM Na<sub>2</sub>CO<sub>3</sub>) containing 4 µg/mL 2C7 (produced in house) or 2 µg/mL anti-His (Thermo Fisher Scientific MA1-21315) overnight at 4 °C. For ELISAs to measure background antibody binding, the plates were coated with 4 µg/mL of polyclonal antibodies isolated from rabbit serum alongside 2 µg/mL anti-His as a positive control. The following day the plates were blocked with 360 µL of PBSMT (PBS containing 2% skim milk powder and 0.05% Tween20) for 30 min at room temperature. Control phage expressing PEP-1 or 6-His peptides were serially diluted in PBSM (PBS containing 2% skim milk powder) and incubated for 30 min at room temperature. The plates were washed 3× with PBST (PBS containing 0.05% Tween20) and 50 µL of anti-M13 HRP diluted 1:20,000 (Sino Biological MM05T) was added in PBSM. After 30 min of incubation the plates were washed a further 3 times before the addition of 50 µL 1-Step™ Ultra TMB-ELISA (ThermoFisher) for less than 10 min. The reaction was quenched with 50 µL 1 M H<sub>2</sub>SO<sub>4</sub> and the plates read at 450 nm on a Spectramax M4. All ELISAs were repeated in triplicate.

### Phage panning

Phage panning was carried out in ELISA 8 well strips (Corning). The wells were coated overnight at 4 °C with 100 µL of purified anti-TeeVax3 antibodies at 4 µg/mL in 50 mM Na<sub>2</sub>CO<sub>3</sub> buffer at pH 9.5 or incubated with Na<sub>2</sub>CO<sub>3</sub> buffer alone. The next day, the solutions were removed, and the plates were blocked with 300 µL PBSMT. After 1 h of shaking at room temperature, the strips were washed 3× with PBST.  $1 \times 10^{11}$  phage per well were then added for 1 h to the strips coated with buffer alone for non-specific phage binding depletion before transfer to the wells coated with antigen. The wells were washed again after 1 h, although the number of washes was increased by three each round to increase selection pressure. Phages were eluted with a 10 min incubation using 100 µL of 0.1 M glycine/HCl pH 2.7, transferred to a 2 mL tube previously blocked with PBS containing 2% skim milk powder, and neutralized with 1 M Tris pH 8.0 at a 1:5 ratio (vol Tris/vol phage). 20 mL SS320 E. coli cells were grown in 2xYT media and 2% glucose medium to an OD 0.4–0.6 at 37 °C without shaking, and incubated with the eluted phages for 30 min at 30 °C. The shaking speed was then increased to 250 rpm for another 30 min. The phage library was recovered by plating infected cells on three 145 mm round LB agar plates containing 2% glucose and 20 µg/mL chloramphenicol and overnight growth at 37 °C.

### Nanopore sequencing and analysis

Library plasmid stocks from each screening phase were directly purified from corresponding E. coli glycerol stocks using via QIAprep Spin Miniprep Kit (Qiagen, Germany). Linear, 723 bp DNA fragments representing the tile library CDS were gel excised and purified with a QIAquick Gel Extraction Kit (Qiagen) following restriction digest of each library plasmid stock with BamHI-HF and XbaI (NEB, USA). Each purified library fragment was then prepared according to the SQK-NBD114.24 Oxford Nanopore Technologies (ONT, UK) ligation sequencing amplicons protocol and kit (200 fmol input), and subsequently sequenced using a R10.4.1 flow cell (ONT). Sequencing was stopped once the estimated raw read count reached  $\geq 100 \times$  coverage per tile per sample.

Base-calling and demultiplexing of raw read data was performed using Dorado (v0.5.3; model dna\_r10.4.1\_e8.2\_400bps\_sup@4.3.0). Read data were filtered for quality control using fastp (v0.23.4<sup>37</sup>) and binned into tile counts via local alignment against the 308 segments using minimap2 (v2.24<sup>38</sup>) and samtools (v1.19.2<sup>39</sup>).

### ELISA analysis for TeeVax3 antibody binding

ELISA analysis was used to compare antibody binding to TeeVax3 with and without the His epitope tag. Antigens were coated overnight at 4 °C on ELISA plates (Corning 3590) at 4 µg/ml in Coating Buffer (50 mM NaHCO<sub>3</sub>, pH 9.5), washed the next day three times with PBST, and blocked with PBSMT. Blocked plates were washed a further three times with PBS Tween20. Serial dilutions of TeeVax3-specific antibodies isolated from rabbit sera were added to the plate, and a goat anti-rabbit IgG HRP antibody (Abcam) was used at 1:50,000 for detection of binding. Control samples confirming His tag removal from the TeeVax3 antigen used a HRP conjugated anti-polyHistidine antibody [HIS-1, Abcam] diluted 1:20,000 in PBSMT. 50 µl 1-Step™ Ultra TMB-ELISA was used for detection of HRP signal in each well and the reaction quenched after 10–15 min with an equal volume of 1 M H<sub>2</sub>SO<sub>4</sub> before reading at 450 nm. All ELISA steps were undertaken at room temperature with incubation periods of 1 h unless otherwise indicated. Fine epitope mapping was performed by ordering synthetic peptides with N-terminal biotin residues (Genscript: 17-mer YHHHHHHHDYDIPTTENL, 14-mer YHHHHHHHDYDIPTT, 13-mer HHHHHHHHDYDIPT, 10-mer HHHHHHHHDYDI, 7-mer YHHHHHHH). ELISA analysis followed the protocol above except the ELISA plates were coated with biotinylated peptides that had been precomplexed with neutravidin at a 4:1 molar ratio for 30 min at room temperature in 50 mM NaHCO<sub>3</sub>, pH 9.5. ELISA data was fit by non-linear regression of a reparametrized 5 parameter logistic model in JupyterLab<sup>40</sup>. All ELISAs were repeated in triplicate. Pairwise t-tests were used to compare data points at each antibody concentration and a Bonferroni correction was applied to account for multiple comparisons.

### Data availability

Processed data and scripts used in this work can be found at [https://github.com/ImmunoLab/2025-peptide\\_tiling](https://github.com/ImmunoLab/2025-peptide_tiling). Raw Nanopore sequencing data is available in the NCBI SRA database under BioProject 1195632 (<http://www.ncbi.nlm.nih.gov/bioproject/1195632>).

Received: 9 December 2024; Accepted: 4 March 2025

Published online: 19 March 2025

### References

- Larocca, R. A. et al. Vaccine protection against Zika virus from Brazil. *Nature* **536**, 474–478 (2016).
- Yihao, L. et al. Robust induction of B cell and T cell responses by a third dose of inactivated SARS-CoV-2 vaccine. *Cell Discov.* **8**, 10 (2022).
- McNamara, H. A. et al. Antibody feedback limits the expansion of B cell responses to malaria vaccination but drives diversification of the humoral response. *Cell Host Microbe* **28**, 572–585.e7 (2020).
- Cao, Y. et al. BA.2.12.1, BA.4 and BA.5 escape antibodies elicited by Omicron infection. *Nature* **608**, 593–602 (2022).
- Sevvana, M. & Kuhn, R. J. Mapping the diverse structural landscape of the flavivirus antibody repertoire. *Curr. Opin. Virol.* **45**, 51–64 (2020).
- Cia, G., Pucci, F. & Rooman, M. Critical review of conformational B-cell epitope prediction methods. *Brief. Bioinform.* **24**, bbac567 (2023).
- Hu, D. & Irving, A. T. Massively-multiplexed epitope mapping techniques for viral antigen discovery. *Front. Immunol.* **14**, 1192385 (2023).
- De Leon, A. J., Tjiam, M. C. & Yu, Y. B cell epitope mapping: The journey to better vaccines and therapeutic antibodies. *Biochim. Biophys. Acta BBA Gen. Subj.* **1868**, 130674 (2024).
- Mohan, D. et al. PhIP-Seq characterization of serum antibodies using oligonucleotide-encoded peptidomes. *Nat. Protoc.* **13**, 1958–1978 (2018).
- Antanasijevic, A. et al. From structure to sequence: Antibody discovery using cryoEM. *Sci. Adv.* **8**, eabk2039 (2022).
- Shrock, E. L., Shrock, C. L. & Elledge, S. J. VirScan: high-throughput profiling of antiviral antibody epitopes. *Bio-Protoc.* **12**, e4464–e4464 (2022).
- Xu, G. J. et al. Viral immunology. Comprehensive serological profiling of human populations using a synthetic human virome. *Science* **348**, aaa0698 (2015).
- Garrett, M. E. et al. Phage-DMS: A comprehensive method for fine mapping of antibody epitopes. *iScience* **23**, 101622 (2020).
- Hanning, K. R., Minot, M., Warrender, A. K., Kelton, W. & Reddy, S. T. Deep mutational scanning for therapeutic antibody engineering. *Trends Pharmacol. Sci.* **43**, 123–135 (2022).
- Loh, J. M. et al. A multivalent T-antigen-based vaccine for Group A Streptococcus. *Sci. Rep.* **11**, 4353 (2021).
- Fan, J., Toth, I. & Stephenson, R. J. Recent Scientific Advancements towards a Vaccine against Group A Streptococcus. *Vaccines* **12**, 272 (2024).
- Raynes, J. M. et al. Identification of an immunodominant region on a group A Streptococcus T-antigen reveals temperature-dependent motion in pili. *Virulence* **14**, 2180228 (2023).
- López-Laguna, H. et al. Insights on the emerging biotechnology of histidine-rich peptides. *Biotechnol. Adv.* **54**, 107817 (2022).
- Zhao, X., Li, G. & Liang, S. Several affinity tags commonly used in chromatographic purification. *J. Anal. Methods Chem.* **2013**, 1–8 (2013).
- Rodrigues, M. X., Yang, Y., de Souza Meira, E. B., do Carmo Silva, J. & Bicalho, R. C. Development and evaluation of a new recombinant protein vaccine (YidR) against *Klebsiella pneumoniae* infection. *Vaccine* **38**, 4640–4648 (2020).
- Otsyula, N. et al. Results from tandem Phase 1 studies evaluating the safety, reactogenicity and immunogenicity of the vaccine candidate antigen Plasmodium falciparum FVO merozoite surface protein-1 (MSP142) administered intramuscularly with adjuvant system AS01. *Malar. J.* **12**, 29 (2013).
- Zang, J. et al. Yeast-produced RBD-based recombinant protein vaccines elicit broadly neutralizing antibodies and durable protective immunity against SARS-CoV-2 infection. *Cell Discov.* **7**, 1–16 (2021).
- Ngampasutadol, J., Rice, P. A., Walsh, M. T. & Gulati, S. Characterization of a peptide vaccine candidate mimicking an oligosaccharide epitope of *Neisseria gonorrhoeae* and resultant immune responses and function. *Vaccine* **24**, 157–170 (2006).
- Krebber, A. et al. Reliable cloning of functional antibody variable domains from hybridomas and spleen cell repertoires employing a reengineered phage display system. *J. Immunol. Methods* **201**, 35–55 (1997).

25. Gulati, S., McQuillen, D. P., Mandrell, R. E., Jani, D. B. & Rice, P. A. Immunogenicity of neisseria gonorrhoeae lipooligosaccharide epitope 2C7, widely expressed in vivo with no immunochemical similarity to human glycosphingolipids. *J. Infect. Dis.* **174**, 1223–1237 (1996).
26. Jumper, J. et al. Highly accurate protein structure prediction with AlphaFold. *Nature* **596**, 583–589 (2021).
27. Qi, H. et al. Antibody binding epitope mapping (AbMap) of hundred antibodies in a single run. *Mol. Cell. Proteomics* **20**, 100059 (2021).
28. Paull, M. L., Bozekowski, J. D. & Daugherty, P. S. Mapping antibody binding using multiplexed epitope substitution analysis. *J. Immunol. Methods* **499**, 113178 (2021).
29. Rajan, J. V. et al. Phage display demonstrates durable differences in serological profile by route of inoculation in primary infections of non-human primates with Dengue Virus 1. *Sci. Rep.* **11**, 10823 (2021).
30. Yaffe, Z. A. et al. Passively acquired constant region 5-specific antibodies associated with improved survival in infants who acquire human immunodeficiency virus. *Open Forum Infect. Dis.* **10**, ofad316 (2023).
31. Singh, M. et al. Effect of N-terminal poly histidine-tag on immunogenicity of *Streptococcus pneumoniae* surface protein SP0845. *Int. J. Biol. Macromol.* **163**, 1240–1248 (2020).
32. Lin, T.-W. et al. Tag-free SARS-CoV-2 receptor binding domain (RBD), but not C-terminal tagged SARS-CoV-2 RBD, induces a rapid and potent neutralizing antibody response. *Vaccines* **10**, 1839 (2022).
33. Przedpelski, A., Tepp, W. H., Pellett, S., Johnson, E. A. & Barbieri, J. T. A novel high-potency tetanus vaccine. *mBio* **11**, e01668-e1720 (2020).
34. Steemson, J. D. et al. Survey of the bp/tee genes from clinical group A streptococcus isolates in New Zealand—Implications for vaccine development. *J. Med. Microbiol.* **63**, 1670–1678 (2014).
35. Falugi, F. et al. Sequence variation in group A *Streptococcus* pili and association of pilus backbone types with lancefield T serotypes. *J. Infect. Dis.* **198**, 1834–1841 (2008).
36. Smith, G. P. & Scott, J. K. Libraries of peptides and proteins displayed on filamentous phage. In *Methods in Enzymology*, vol. 217, 228–257 (Academic Press, 1993).
37. Chen, S. Ultrafast one-pass FASTQ data preprocessing, quality control, and deduplication using fastp. *iMeta* **2**, e107 (2023).
38. Li, H. New strategies to improve minimap2 alignment accuracy. *Bioinformatics* **37**, 4572–4574 (2021).
39. Danecek, P. et al. Twelve years of SAMtools and BCFtools. *GigaScience* **10**, giab008 (2021).
40. Liao, J. J. Z. & Liu, R. Re-parameterization of five-parameter logistic function. *J. Chemom.* **23**, 248–253 (2009).

# Acknowledgements

This work was supported by an MWC project grant (#4026) that also supported K.BC with a Masters Scholarship. K.H. was supported by a University of Waikato Doctoral scholarship. W.K. was supported by a New Zealand Marsden Grant (23-UOW-006).

### Author contributions

K.B.C. and K.R.H. contributed equally to this work. K.R.H., J.L., and W.K. conceived of and designed the study. K.B.C., K.R.H., K.B., and M.R. performed laboratory experiments and created reagents used in the study. K.R.H. and K.B.C. performed the Nanopore sequencing and bioinformatic analysis. K.R.H., K.B.C., and W.K. wrote the manuscript. All authors provided feedback and revisions for the final version of the manuscript.

### Declarations

### Competing interests

The authors declare no competing interests.

### Additional information

**Supplementary Information** The online version contains supplementary material available at <https://doi.org/10.1038/s41598-025-92928-3>.

**Correspondence** and requests for materials should be addressed to W.K.

**Reprints and permissions information** is available at [www.nature.com/reprints](http://www.nature.com/reprints).

**Publisher's note** Springer Nature remains neutral with regard to jurisdictional claims in published maps and institutional affiliations.

**Open Access** This article is licensed under a Creative Commons Attribution-NonCommercial-NoDerivatives 4.0 International License, which permits any non-commercial use, sharing, distribution and reproduction in any medium or format, as long as you give appropriate credit to the original author(s) and the source, provide a link to the Creative Commons licence, and indicate if you modified the licensed material. You do not have permission under this licence to share adapted material derived from this article or parts of it. The images or other third party material in this article are included in the article's Creative Commons licence, unless indicated otherwise in a credit line to the material. If material is not included in the article's Creative Commons licence and your intended use is not permitted by statutory regulation or exceeds the permitted use, you will need to obtain permission directly from the copyright holder. To view a copy of this licence, visit <http://creativecommons.org/licenses/by-nc-nd/4.0/>.

© The Author(s) 2025